

## Comparative Study of Pore Size of Low-Dielectric-Constant Porous Spin-on-Glass Films Using Different Methods of Nondestructive Instrumentation

Eiichi KONDOH\*, Mikhail R. BAKLANOV<sup>1</sup>, Eric LIN<sup>2</sup>, David GIDLEY<sup>3</sup> and Akira NAKASHIMA<sup>4</sup>

*Department of Mechanical System Engineering, Faculty of Engineering, Yamanashi University, 4-3-11 Takeda, Kofu 400-8511, Japan*

<sup>1</sup>*Silicon Processing Technology Division, IMEC, Kapeldreef 75, 3001 Leuven, Belgium*

<sup>2</sup>*Materials Science and Engineering Laboratory, National Institute of Standards and Technology, Gaithersburg, Maryland 20899, U.S.A.*

<sup>3</sup>*Department of Physics, University of Michigan, Ann Arbor, Michigan 48109, U.S.A.*

<sup>4</sup>*Fine Chemicals Research Center, Catalysts and Chemicals Industry Co. Ltd., Wakamatsu, Kitakyushu, Fukuoka 808-0027, Japan*

(Received January 5, 2001; accepted for publication February 16, 2001)

The pore sizes of hydrogen-methyl-siloxane-based porous spin-on-glass (SOG) thin films having different  $k$  values ( $k = 1.8$ – $2.5$ ) are comparatively studied using different nondestructive instrumental ways and also with reference to sorption porosimetry. The pore size and its spread are found to increase with increasing porosity, or with decreasing dielectric constant.

**KEYWORDS:** low-dielectric-constant films, pore size distribution, ellipsometry, neutron scattering, positronium annihilation

Resistance-capacitance (RC) delay in the multilevel interconnections of ultralarge-scale integrated circuits (ULSIs) has become the determining factor in overall chip performance. This is due to continuous miniaturization of interconnects, more specifically, to wiring elongation that increases the conductor resistance as well as to the reduction in conductor spacing that increases parasitic capacitance and signal crosstalk. To mitigate this problem, the ULSI industry urgently demands new materials that have a lower dielectric constant ( $k$ ) for use in interlayer and intermetal insulation layers.

The use of porous dielectric films is of considerable interest in the ULSI metallization community to obtain the ultimate dielectric constant near unity.<sup>1–3</sup> Among the many candidates of porous media, silica-based spin-on-glasses (SOGs) have been thought to be the most feasible because of their potential compatibility with conventional Si technology and also because of the high thermal and mechanical stability of the backbone siloxane network.

Pore size and its distribution are crucial properties of porous low- $k$  materials. The maximum pore size must be sufficiently smaller than the minimum feature size of device components. A too widely spread pore size distribution (PSD) could result in film nonuniformity and poor process controllability. Properties important in practical applications, such as mechanical strength, electrical and thermal stability, and thermal conductivity are closely related to the structure of the SOG backbone. Characterization of pore size helps to have better understanding of the backbone structure and to improve these properties.

There are many known established methods for determining the pore size and PSD of porous media, such as mercury porosimetry and sorption porosimetry. These methods are based on the permeation of a probe substance—usually liquid or gas—into the pores. The amount of permeation is measured against the operative parameter, pressure for instance, and then the acquired data is transformed to obtain information on pore size. In order to determine the PSD and average/mode pore size, measurement of a small variation in the degree of permeation against the change of the operative parameter is required. This is because the derivation of a distribution curve is essentially a differential operation. The conventional porosimetries are hardly applicable to thin films, be-

cause thin films have too small a total pore volume and surface area which result in too little sorption. Nevertheless necessary, one needs to scrape off the films from a few tens of wafers to obtain a sufficient amount of specimen.

Recently, advanced nondestructive methods, such as ellipsometric porosimetry (EP),<sup>4</sup> small-angle neutron scattering spectroscopy (SANS) combined with specular X-ray reflectivity (SXR),<sup>5</sup> and positronium annihilation lifetime spectroscopy (PALS),<sup>6</sup> have been successfully applied to determine the pore size and PSD of low- $k$  porous thin films. Although these new techniques are based on different physicochemical principles, to our knowledge, few systematic studies have been thus far reported on crossover experiments using the same specimens.

In this Letter, we report on EP, SANS/SXR, PALS and conventional N<sub>2</sub> porosimetry results obtained comparatively from the same set of low- $k$  porous SOG films. Four types of SOGs with different porosities are used in order to perform reliable experiments and to study the effect of porosity on pore size and PSD.

Hydrogen-methyl-siloxane-based porous SOGs, synthesized from silicon alkoxides, silica sol, and a pyloric composite polymer, are formed on Si wafers. The composite polymer dissipates during the final cure (450°C for 30 min in nitrogen), leaving small pores. The silica sol particles are interconnected in the siloxane network. Details about this type of SOG are documented elsewhere.<sup>7</sup> Four different precursor solutions were prepared to have different mixing ratios of the pyloric porosity template so that four types of SOG films are formed. Table I summarizes the film properties used in this work. The dielectric constants are 1.8–2.5. The wafers are divided into pieces and are subjected to different instrumental analyses of pore size. As stated above, four different methods are used in the present round robin experiments. Two of these methods

Table I. Properties of the films measured on-site.

Sample	Refractive Index (633 nm)	Thickness (Å)	Dielectric Constant (1 MHz)
RR18	1.198	2549	1.8
RR20	1.223	4029	2.0
RR22	1.257	4172	2.2
RR25	1.317	3973	2.5

\*E-mail address: kondoh@ccn.yamanashi.ac.jp

are sorption porosimetries, namely EP<sup>4)</sup> and Barrett-Joyner-Halenda (BJH) N<sub>2</sub> porosimetries,<sup>8,9)</sup> and the others are radiation beam-based, spectroscopies, namely SANS/SXR<sup>5)</sup> and PALS.<sup>6)</sup> Bulk specimens are used only in the BJH porosimetry, i.e., it is film-destructive. Note that about twenty 8-inch wafers are needed to obtain one bulk specimen. We do not further state the experimental setup for simplicity. Details are well documented in the literature. The principle of each method is however described briefly along with the experimental results in order to facilitate understanding.

The results are summarized in Table II. The porosity is determined in the EP and SANS/SXR experiments, and the film thickness is determined using EP and SXR. Characteristic pore size has practically the same meaning as pore diameter as defined in conventional porosimetry. The term *diameter* is not used, because the pore model geometry is not always characterized by a circle.

The primary parameter measured by sorption porosimetry is the amount of adsorbed substance. The PSD is determined from capillary and layer condensation theories of gaseous adsorptive.<sup>8)</sup>

The EP is based on an *in-situ* ellipsometric measurement carried out to detect a small change of optical film parameters ( $\Delta$  and  $\Psi$ ) upon sorption—toluene in our case. Figure 1 shows the PSDs obtained by EP for specimens RR18–RR25. The specific surface area at a given pore diameter,  $dV/dD$ , has a sharp peak, and the peak pore diameter increases as  $k$  increases. The peak spread is observed to decrease with increasing  $k$ . Average pore diameters are shown in Table II. The trend is the same as that of the peak pore diameter, i.e., the average pore diameter increases as  $k$  decreases. However, RR18 has a much smaller pore size than RR20.

The BJH N<sub>2</sub> porosimetry, being regarded as a standard technique for mesoporosity characterization, is carried out using a Quantachrome Autosorb-6 sorption analyzer. The average pore diameter obtained show good agreement with the EP data, including the inversion of pore diameters of RR18 and RR20. Cumulative pore volumes are 0.98, 0.88, 0.70 and 0.35 (ml/g) for RR18, RR20, RR22 and RR25, respectively, which shows consistent agreement with the change of  $k$ .

Conventional methods of sorption porosimetry such as the N<sub>2</sub> sorption porosimetry is not capable of detecting inaccessible (closed) pores, because the adsorptive vapor is not accessible to the closed pores. A unique feature of the EP is wherein the amount of the closed pores can be determined with a multiangular and/or spectroscopic ellipsometry arrangement assuming a dielectric model that the film consists of solid part (wall) + open porosity filled with adsorptive + closed pore (void). The refractive index of the wall material determined by multiangular EP is about 1.422, which is very close to the value of a condensed hydrogen-methyl-siloxane bulk specimen.<sup>10)</sup> It is found that the pore connectivity, the ratio of open porosity to total porosity, increases from 86% (RR25) to 97% (RR18) as  $k$  decreases. The determined full porosity (listed in Table II) is observed to consistently increase as  $k$  decreases.

In the radiation beam-based porosimetry techniques—SANS/SXR and PALS—the signal from the specimen is analyzed. The primary beam interacts with pores and/or wall materials and bears the information of the pore structure. The pore size is extracted from the measured signal, assuming pore geometry and physical interaction between the beam and

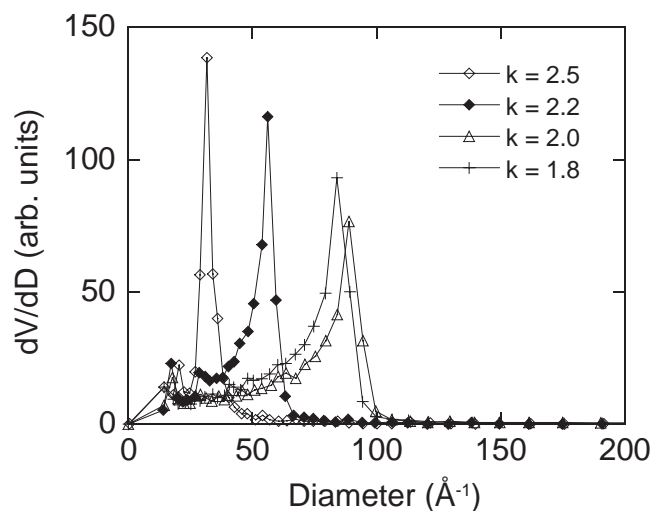


Fig. 1. Pore size distributions of porous SOG films obtained by ellipsometric porosimetry.

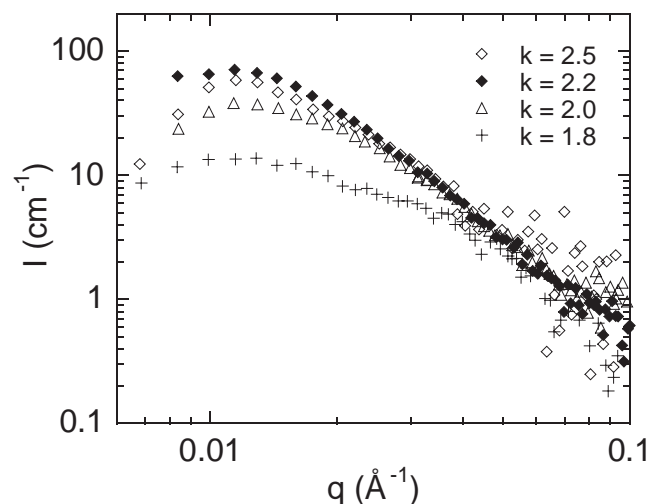


Fig. 2. Small-angle neutron scattering intensity,  $I$ , versus scattering vector,  $q$  for porous SOG films.

pore.

In SANS/SXR experiments, Rutherford backscattering spectrometry (RBS) and forward recoil elastic scattering (FRES) are also employed, and film thickness, wall density, overall film density, porosity, average pore chord length (pore size), and elemental composition are characterized.

Figure 2 shows the absolute scattered neutron intensity,  $I$ , plotted against the scattering vector ( $q$ ) where  $q = (4\pi/\lambda) \sin(\theta/2)$ , and  $\theta$  is the scattering angle from the incident beam path and  $\lambda$  is the neutron wavelength (6 Å). The form and magnitude of the scattered intensity is a function of the film porosity, pore size, wall density, and elemental composition. For these samples, the scattering data from each sample are well described by the random two-phase model of Debye.

Quantitative analyses are carried out in the following manner.<sup>5)</sup> The SANS intensity data as a function of  $q$  is a function of the porosity and wall density. The function form is determined assuming a random two-phase (void + solid) structure. The film thickness and overall electron density are evaluated by the SXR measurements and are combined with the film

Table II. Summary of PSD analysis.

Sample	Characteristic Pore Size (Å)				Porosity (%)		Thickness (nm)	
	EP	BJH	SANS/SXR	PALS	EP	SANS/SXR	EP	SXR
RR18	84	70	62	82	53	37	265	265
RR20	90	92	61	73	45	33	418	424
RR22	57	63	50	57	39	26	427	424
RR25	31	33	27	39	26	20	410	427

composition data obtained by RBS and FRES so that the overall film density is determined. Since the overall film density is also a function of porosity and wall density, these values are independently obtained by solving for the unknowns in the equations from SANS and SXR. The results are shown in Table II. It is apparent that the average pore size increases with increasing porosity. These pore size values are similar to those obtained from the sorption porosimetry measurements. It is also observed that the average film density decreases with increasing porosity (1.082, 0.939, 0.833, and 0.727 (g/cm<sup>3</sup>) for RR25, RR22, RR20, and RR18, respectively). Film thickness data calculated from SXR are in good agreement with the data from EP, where the difference is within 4%.

In PALS, films are irradiated with a focused positron beam. Positron forms positronium—the electron-positron bound state—that is trapped in the pores where its natural lifetime of 142 ns is reduced by annihilation during collisions with the pore surfaces. Thus, the reduced lifetime can be correlated with pore size.

Positronium lifetime histograms are recorded, and the lifetime distribution curves are obtained with a fitting program specific for this purpose. The distribution curves are transformed into pore size data, using pore geometries of three-dimensional cubes or two-dimensional infinitely long-square-channels.<sup>6)</sup> It is noted that the discrepancy between the two models is not very significant.

The PALS data shown in Table II are deduced using an infinitely long square channel pore model, where the pore size is the side length corresponding to a tubular pore diameter. The pore size increases with decreasing  $k$ , and the values are very similar to those obtained by other techniques. In all four films, the pores are found to be nominally fully interconnected.

A crucial objective of this study is to demonstrate specific tendencies and characteristics of the pore data obtained by different methods. The instrumental methods employed in this study are based on different physicochemical principles. The pore sizes are not directly acquired from the measurements. In order to determine the pore size and porosity, it is necessary to transform the raw data by assuming an appropriate model that takes into account the pore structure and pore-probe interaction. That is, the results are highly model dependent. Sorption porosimetry is reflected by the pore surface geometry and SANS is reflected by the spatial density of scattering bodies, either voids or particles. PALS is more related to the volume of void elements. For these reasons, we must emphasize that a perfect agreement between the results cannot be obtained. To provide calibration data or to carry out screening tests is not the scope of this study.

Other than the above points, it can be safely said that a successful agreement is obtained. The difference in the pore sizes obtained using different methods is not very significant. The

dependence of porosity on  $k$  is reasonable. It is also found that the spread of pore size increases with average/mode pore size. To investigate the dependence of the pore parameters on porosity is, in fact, another scope of this work. Porosity is more or less predictable from  $k$ . However, the pore size and PSD cannot be uniquely determined by  $k$ . The consistency among porosity, pore size, its spread, and  $k$  is observed regardless of experimental methods used. Therefore, it is concluded that the porosity can be used as a representative measure of PSD, more specifically, average pore size for silica-based porous SOG thin films synthesized through sol-gel methods.

However, a small inconsistency is observed in the data of RR18 and RR20. Both EP and BJH data show that RR18 has a smaller pore size than RR20. The SANS/SXR data show that these specimens have almost identical pore sizes. However, RR18 has the largest pore size in the PALS analysis. This discrepancy may reflect the limitation of pore analysis techniques when pore size and/or PSD is large. Some of the authors are now in the process of collecting more data of various porous thin films synthesized by different methods.

EP, BJH porosimetry, SANS/SXR, and PALS are comparatively used to evaluate pore size and porosity of hydrogen-methyl-siloxane-based porous spin-on-glass (SOG) thin films having different  $k$  values ( $k = 1.8$ – $2.5$ ). The porosity and pore size data show good agreement regardless of the instrumental methods used for measurement. The pore size and its spread are found to increase with increasing porosity, or with decreasing  $k$ . This implies that porosity can be used as a representative measure of pore size distribution. From a methodology point of view, we conclude that any methods employed in this study are appropriate for characterizing pores.

The authors are grateful for the considerable contribution to this round robin project made by H. Arao and K. Nakayama (CCIC) for the precursor synthesis and film preparation, H.-J. Lee (NIST) for the SANS/SXR measurements, and K. P. Mogilnikov (Institute for Semiconductor Physics, Novosibirsk, Russia) and D. Shamiryan (IMEC) for the EP measurements. They also would like to thank all of them for useful discussions.

- 1) K. Endo: MRS Bull. **22** (1997) 55.
- 2) R. S. List, A. Singh, A. Ralston and G. Dixit: MRS Bull. **22** (1997) 61.
- 3) N. Aoi: Jpn. J. Appl. Phys. **36** (1997) 1355.
- 4) M. R. Baklanov, K. P. Mogilnikov, V. G. Polovinkin and F. N. Dultsev: J. Vac. Sci. & Technol. B **18** (2000) 1385.
- 5) W.-I. Wu, W. E. Wallace, E. K. Lin, G. W. Lynn, C. J. Glinka, E. T. Ryan and H. M. Ho: J. Appl. Phys. **87** (2000) 1193.
- 6) D. W. Gidley, W. E. Frieze, T. L. Dull, J. Sun, A. F. Yee, C. V. Nguyen and D. Y. Yoon: Appl. Phys. Lett. **76** (2000) 1282.
- 7) R. Muraguchi, M. Egami, H. Arao, A. Tonai, A. Nakashima and M. Komatsu: Mater. Res. Soc. Symp. Proc. **565** (1999) 63.
- 8) S. M. Gregg and K. S. W. Sing: *Adsorption, Surface Area & Porosity*

(Academic Press, London, 1982) 2nd ed.

- 9) Being strictly, the BJH porosimetry is a type of sorption porosimetry that uses the BJH sorption theory and Kelvin condensation theory to correlate the amount of sorption and pore size. In this sense, the BJH porosimetry is not limitedly applied to bulk specimens. In order to dis-
- 10) D. Shamiryam, K. Mogilnikov, I. Leonov and M. R. Baklanov: private communication.

tinguish this method from the nondestructive porosimetry techniques, we use this terminology to specify the use of bulk specimens.